

Effect of oxidation temperature on the corrosion response of anodic coatings on Ti6Al4V alloy

Efecto de la temperatura de oxidación en la respuesta a la corrosión de los recubrimientos anódicos en la aleación de Ti6Al4V

Janer Orozco-Rodriguez¹, Ana Fonseca-Reyes², Mauricio Márquez Santos¹, Evert de los Ríos Trujillo³, José Escorcía-Gutiérrez^{4,5}, Roosvel Soto-Díaz^{1,5}

¹MEng. Ingeniería Mecánica, Universidad Autónoma del Caribe, Grupo de investigación IMTEF, Barranquilla, Colombia

ORCID: <https://orcid.org/0000-0001-8282-4844> Email: janer.orozco@uac.edu.co

ORCID: <https://orcid.org/0000-0002-4251-2990> Email: mauricio.marquez45@uac.edu.co

ORCID: <https://orcid.org/0000-0003-4897-398X> Email: roosevelt1019@gmail.com; roosvel.soto@uac.edu.co

²MSc. Ingeniería Mecánica, Universidad del Norte, Grupo de investigación en Materiales, Procesos y Diseño, Barranquilla, Colombia

ORCID: <https://orcid.org/0000-0003-4926-2426> Email: fonsicama@uninorte.edu.co

³MEng. Telemática, Universidad Autónoma del Caribe, Grupo de investigación IET-UAC, Barranquilla, Colombia

ORCID: <https://orcid.org/0000-0003-0268-4381> Email: evert.delosrios23@uac.edu.co

⁴MSc. Ingeniería Electrónica, Universidad Autónoma del Caribe, Grupo de investigación IET-UAC, Barranquilla, Colombia

⁵MSc. Ingeniería Electrónica, Escuela Naval de Suboficiales A.R.C. "Barranquilla", Grupo de investigación GITIN, Barranquilla, Colombia

ORCID: <https://orcid.org/0000-0003-0518-3187> Email: joshesc@gmail.com

Recibido: 10/12/2020

Aceptado: 18/01/2021

Cite this article as: J. Orozco-Rodriguez, A. Fonseca-Reyes, M. Márquez, E. de los Ríos, J. Escorcía-Gutiérrez y R. Soto-Díaz "Effect of oxidation temperature on the corrosion response of anodic coatings on Ti6Al4V alloy", Prospectiva, Vol 19, N° 2, 2021.

<https://doi.org/10.15665/rp.v19i2.2594>

ABSTRACT

In this article, the effect of thermal oxidation temperature on Ti6Al4V alloy anodized coatings by corrosion response was evaluated using potentiodynamic, open-circuit potential (OCP), and electrochemical impedance spectroscopy (EIS) tests. in a 3.5% NaCl solution. For the methodological development, optical microscopy and scanning electron microscopy were used to study and relate microstructural evolution with the analysis of corroded regions. Digital image analysis allows estimating the temperature increases in the porous layer of TiO₂ that occur in the increase in corrosion resistance. The results on the condition of the

TiOX560°C were presented with a higher resistance to corrosion compared to the base metal and other conditions. From the digital image processing it was possible to estimate the possible growth of the porous layers rich in TiO₂, increasing the corrosion resistance of the heat-treated samples considered to the base metal.

Keywords: Ti6Al4V, Thermal oxidation, EIS, TiO₂, Corrosion, Image analysis

RESUMEN

En este artículo, se evaluó el efecto de la temperatura de oxidación térmica en los revestimientos anodizados de aleación de Ti6Al4V por la respuesta a la corrosión mediante las pruebas potenciodinámicas, de potencial de circuito abierto (OCP) y de espectroscopia de impedancia electroquímica (EIS) en una solución de NaCl al 3,5%. Para el desarrollo metodológico se utilizaron la microscopía óptica y la microscopía electrónica de barrido para estudiar y relacionar la evolución microestructural con el análisis de las regiones corroídas. El análisis de imágenes digitales permite estimar los aumentos de temperatura en la capa porosa de TiO₂ que se producen en el aumento de la resistencia a la corrosión. Los resultados sobre la condición del TiOX560° se presentaron con una mayor resistencia a la corrosión en comparación con el metal base y otras condiciones. A partir del procesamiento de imágenes digitales se pudo estimar el posible crecimiento de las capas porosas ricas en TiO₂ aumentando la resistencia a la corrosión de las muestras tratadas con calor consideradas al metal base.

Palabras clave: Ti6Al4V, Oxidación térmica, EIS, TiO₂, Corrosión, Análisis de imágenes

1. INTRODUCTION

Titanium is the fourth most abundant structural metal, and its properties have made it the material of choice in many industries such as aerospace (blades), biomedical (prosthetics), automotive (connecting rods, springs) due to its excellent mechanical strength and its corrosion resistance in a wide variety of environments [1]. Forming a thin film of oxide passive self-adhering on their surfaces is considered responsible for this attribute. However, the corrosion rate of titanium and its alloys is significant when exposed to aggressive media. Surface modification is a promising method for increasing the surface hardness, corrosion resistance, and wear resistance of titanium and its alloys [2]. For many of these applications, it is crucial to maximizing the specific surface area (e.g., evident for any catalytic reaction) to achieve maximum overall efficiency. Nanotubes oxide film formation is generated, which improves the corrosion resistance of titanium, but if desired to increase the said layer's thickness, there is a surface treatment complementary called thermal oxidation [3, 4].

Assuming the importance of TiO₂ nanostructures, we focus on a complementary process known as thermal oxidation, which is seen as a cost-effective method to deliberately generate a relatively thicker barrier oxide layer on titanium compared to the naturally formed oxide layer. Moreover, the thermal oxidation of titanium aims to produce ceramic coatings, mainly rutile-based, in the form of a crystalline oxide film, accompanied by the dissolution of oxygen underneath them. The thermally formed oxide layer allows an increase in hardness, wear-resistance, and corrosion resistance. Thermally oxidized titanium nanostructures show a higher content of rutile and greater resistance to corrosion due to the increase in the surface of the matrix of the nanostructures. There is also a more excellent stability of the crystalline structure, and a passive oxide layer is formed below the nanostructure matrix [5, 6].

This work aims to determine the effect of oxidation temperature on anodic coatings' corrosion response on Ti6Al4V alloy. The proposed work achieves free anodized defects and thermally oxidized samples at different temperatures, developing microstructural analyzes, corrosion tests based on electrochemical impedance tests, and digital image analysis.

The following paper is organized as follows: experimental procedure exposed the experimental procedure developed for this investigation. Afterward, the results and discussion are presented in section 3. Finally, conclusions explain the main conclusions as well as future experimentations of this work.

2. EXPERIMENTAL PROCEDURE

For the development work, the selection of parameters for the anodizing and thermal oxidation is initially performed based on literature and thus able to conduct tests Electrochemical impedance (Open Circuit Potential, Curves Potentiodynamic, Bode and Nyquist plots). Additionally, and as support of the electrochemical tests, the images obtained were analyzed by optical microscopy, scanning electron microscopy and image analysis method OTSU.

2.1. Material

The metal used in the anodizing and thermal oxidation procedure was Ti6Al4V titanium alloy with a thickness of 3mmx10mm and a chemical composition shown in Table 1 for analyzing the initial behavior.

Table 1. Chemical Composition (wt%) of Ti6Al4V.

Tabla 1. Composición química (wt%) del Ti6Al4V.

<i>Ti6Al4V</i>	<i>Al</i>	<i>V</i>	<i>Fe</i>	<i>C</i>	<i>O</i>	<i>N</i>	<i>H</i>	<i>Ti</i>
UNE-7301	5.5 – 6.50	3.5 – 4.50	0.25	0.08	0.13	0.05	0.01	Bal
ISO 5832-3	5.5 – 6.75	3.5 – 4.50	0.30	0.08	0.20	0.05	0.01	Bal
ASTM F136	5.5 – 6.50	3.5 – 4.50	0.25	0.08	0.13	0.05	0.01	Bal

2.2 Process parameters and performance

Process parameters and performance. Before the anodization process, the samples were mechanically polished with alumina (0.05 μm) and chemically etched with 3% dilute Nital acid to remove the surface layer of oxide in the samples that form spontaneously before the electrochemical process is applied.

For the anodizing process, the chemical composition used was: $\text{H}_3\text{PO}_4 + 0.2\text{wt}\%$ HF 1M and executed for a time of 60 seconds. The samples were rinsed in distilled water and air-dried. Then, anodization was carried out in a two-electrode cell at a constant voltage of 14V in an electrolyte of $\text{H}_3\text{PO}_4 + 0.2\text{wt}\%$ HF 1M at 25 °C for 60 minutes. An AISI-SAE304 stainless steel plate was used as the cathode.

After the anodizing process, the thermal oxidation process was carried out to increase the protective layer with the conditions shown in table 2. For thermal oxidation, the samples were heat treated at temperatures of 480°C, 560°C, and 640°C with a heating rate of 5°C/min and a subsequent holding time of 2 hours with a cooling rate in the oven (2°C per minute). The specimens were removed from the oven approximately 24 hours after the process started. Table 2 consolidates the experiments carried out.

Table 2. Summary of the conditions evaluated in thermal oxidation.

Tabla 2. Resumen de las condiciones evaluadas en la oxidación térmica.

Sample	Temperature	Time	Heating rate	Cooling rate	Cooling medium
Base metal (Ti6Al4V)	-	-	-	-	-
TiOx480°C	480°C (753K)	2 hours	5°C/min	2°C/min	Furnace
TiOx560°C	560°C (833K)	3 hours	5°C/min	2°C/min	Furnace
TiOx640°C	640°C (913K)	4 hours	5°C/min	2°C/min	Furnace

2.3. Corrosion test

Open Circuit Potential, potentiodynamic polarization, and electrochemical impedance spectroscopy (EIS) measurements of Ti6Al4V alloy and surface-modified samples were carried out using a Gamry 600@

Electrochemical Workstation. The curves started from -0.3V (vs. OCP) to $+3\text{V}$ (vs. Ag/AgCl, saturated KCl) at a constant scan rate of 0.16 mV per second. The corrosion current density (A/cm^2) was used to determine the different samples' corrosion kinetics.

For Electrochemical Impedance Spectroscopy (EIS), the frequency range was 100 kHz to 10 MHz with an AC amplitude of 5 mV . Spectrum was processed using an equivalent circuit of Double Randles. Corroded samples were observed and analyzed by scanning electron microscopy JOEL 5910LV ® and digital image analysis from the adjustable binarization process.

3. RESULTS AND DISCUSSION

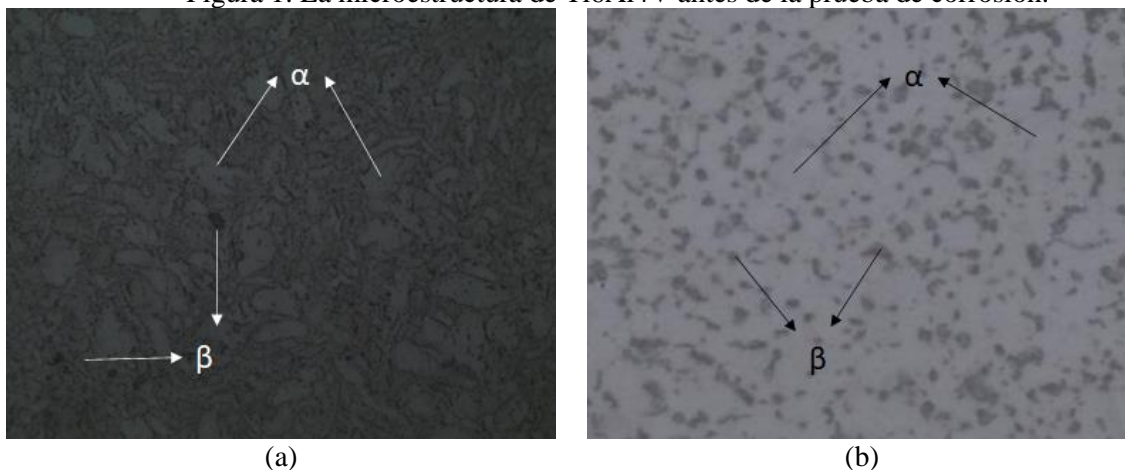
The results showed the initial condition of the base metal prior to the electrochemical tests, which provided a basis for the behavior presented for the surface modification and electrochemical tests. Secondly, the electrochemical tests were carried out which showed the resistance to corrosion of the different oxidation temperatures. Finally, the micrographic analysis by SEM in conjunction with the image analysis correlated the corrosion behavior with its oxidation morphology.

3.1. Microstructural observations

Microstructure characterization results of base metal in as-received state denote the α (alpha) matrix was distinguished in white color, and the contained β (beta) phase of dark gray color, where the less light parts make up the β phase of the structure and the more illuminated parts refer to the α matrix [5].

In the micrograph from the longitudinal section in Figure 1 (a) can be seen grains are elongated attributable to the deformation to which the material is subjected in its manufacturing process, while the micrograph of the cross-section in Figure 1 (b) presents a standard form grain (parallel). Therefore, it can be assured that it is like a grain equiaxial morphology and with a uniform structure throughout the dendrites with grain boundaries thick enough in their endings [6, 7].

Figure 1. Ti6Al4V Microstructure before the corrosion test.
Figura 1. La microestructura de Ti6Al4V antes de la prueba de corrosión.



3.2. Electrochemical test

In the measurement of open circuit potential (OCP), Figure 2 (a) of the variation of the base metal potentials and each condition of surface modification is observed. Initially, the condition with the highest potential was TiOx560°C. Stable values of the modified materials' open circuit potentials are also observed (480°C, 560°C, and 640°C), ranging between -0.127V and 0.027V for the different conditions.

The values start with the base metal that presented an average value of -0.254V, similar to the one studied by [8], an average of -0.30V. The open-circuit potential values in the surface modified materials decreased widely concerning the base metal, as shown in Figure 2 (a), representing a significant improvement in the base metal's corrosion behavior. Therefore, it is known that during anodization and thermal oxidation, an increase in the formation of porous TiO₂ was generated on the surface of the titanium sample, which changes its potential with reference to the base metal, moving towards a noble direction, which increased its resistance to corrosion [6].

These values present behavior that increases depending on the surfaces. When making surface modifications such as anodizing and thermal oxidation, the potentials improve, similar to that presented in other research works [9].

Figure 2. (a) Open circuit potential and (b) Potentiodynamic polarization curves measured in base metal, TiOX480°C, TiOX560°C, and TiOX640°C.

Figura 2. (a) Potencial de circuito abierto y (b) Curvas de polarización potenciodinámica medidas en el metal base, TiOX480°C, TiOX560°C y TiOX640°C.

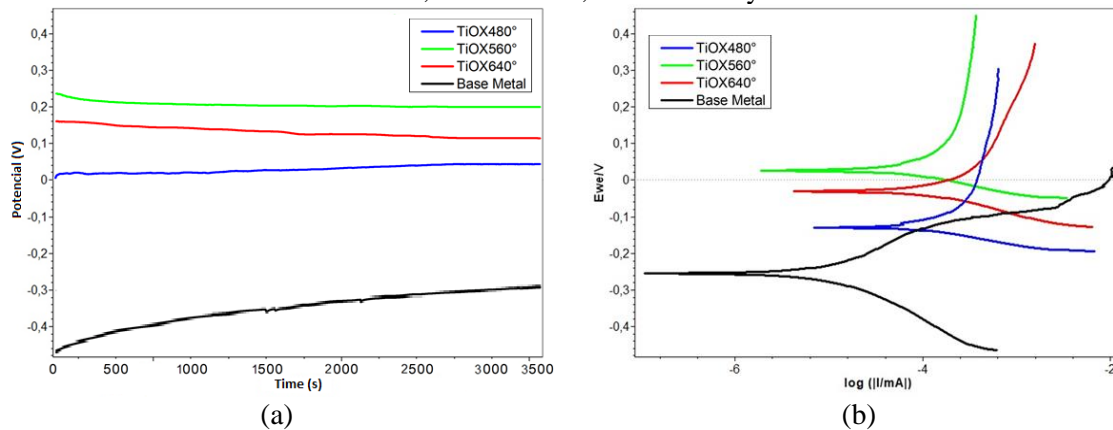


Figure 2 (b) and Table 4 are shown potentiodynamic test results from base metal and each condition of surface modification. Results show the anodic and cathodic branches to the modified conditions; however, different behavior occurs superficially in the base metal [10, 11]. The anodic branch of the polarization curve exhibits an active-passive transition in all the cases of thermal oxidation. However, the active region of the polarization curves of the thermally oxidized Ti6Al4V alloy is extended towards the lower current region, suggesting the ability of the thermally formed oxide layer to offer an improvement in corrosion resistance.

The outcomes exhibited that the E_{corr} (corrosion potential) in the thermally oxidized samples is nobler than the base metal. Potentiodynamic curves indicated that thermal oxidation generated accelerated TiO₂ layer growth, so all the conditions evaluated showed an impairment in the corrosion resistance but superior in corrosion resistance compared to the base metal [10]. This is evidenced by the decrease in I_{corr} which is directly proportional to the corrosion. Given the above, the condition has shown that TiOX560°C possibly

presents the TiO₂ layer generated by thermal oxidation is thicker than the other conditions with higher corrosion resistance.

According to the other investigations, the passivation current decrease of thermally oxidized Ti6Al4V alloy suggests that the oxide film formed on its surface possesses a better insulating property and makes it difficult to pass higher currents for increased chemical reaction/oxidation of species in the electrolyte [5].

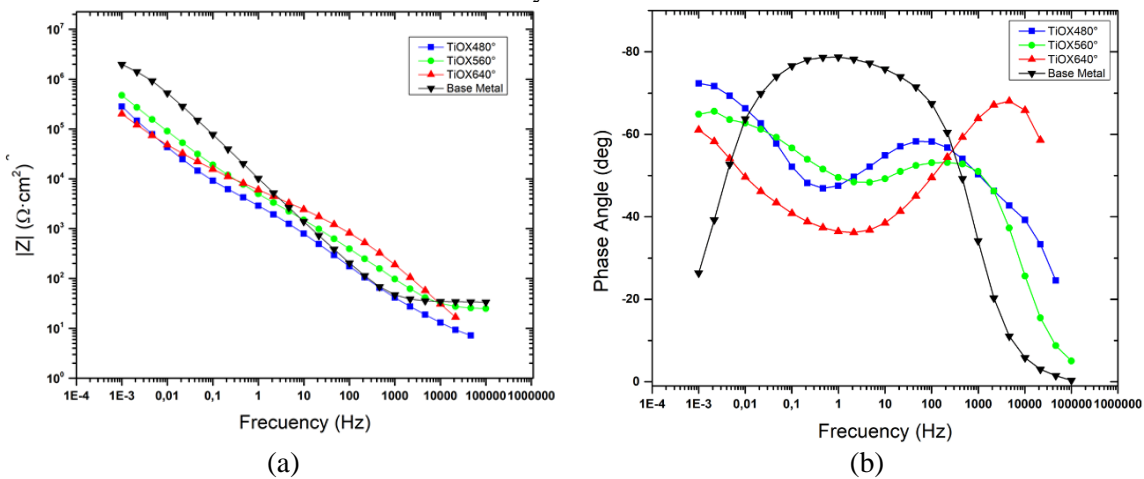
Table 3. Corrosion test data.
 Tabla 3. Datos de la prueba de corrosión.

Sample	E _{corr} (V)	I _{corr}
Base metal (Ti6Al4V)	- 0.254	0.004
TiO _x 480°C	-0.127	0.057
TiO _x 560°C	0.027	0.040
TiO _x 640°C	-0,030	0.068

Figure 3 shows the Bode magnitude and Bode Phase plots of the EIS measurements, respectively in a) and b). The selected equivalent circuit is observed in Figure 4 b), which was selected considering a reasonable approximation to the behavior of thermal oxidation and anodization, which are corrosion inhibitors. Thus, an equivalent circuit model (Figure 4 d)) consisting of solution resistance (R_s), charge transfer resistance (R_{ct}), film resistance (R_f), and constant phase elements (CPE and CPE1) were applied to analyze the EIS data.

Figure 3. Images show (a) Bode Magnitude and (b) Bode Phase of the anodized and thermally oxidized samples.

Figura 3. Las imágenes muestran en (a) Magnitud de Bode y en (b) Fase de Bode de las muestras anodizadas y oxidadas térmicamente.

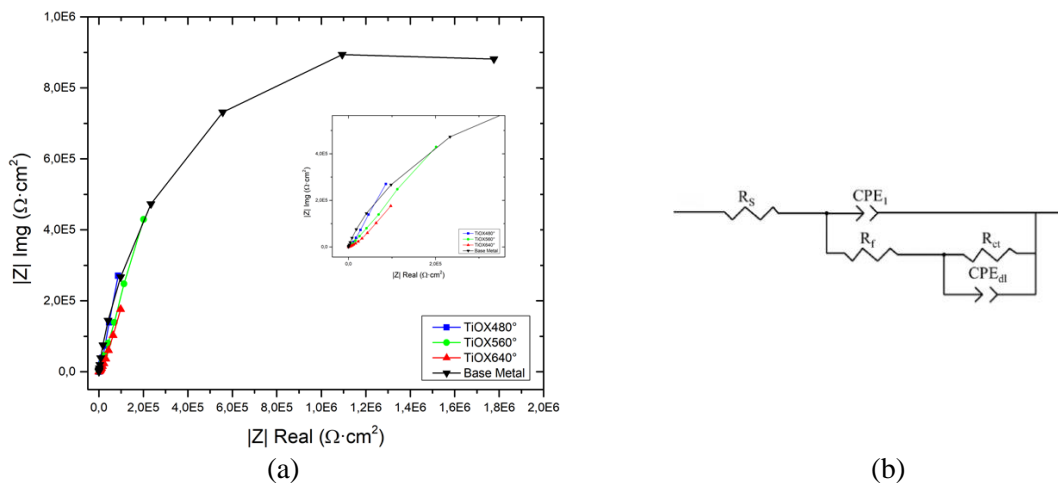


The analysis of Bode's results shows that the base metal has a superior behavior in terms of corrosion resistance, that is, greater impedance. On the other hand, from the thermally oxidized conditions, especially TiOX560°C, it presented higher impedance values compared to the other conditions and similar to the Base Metal. A high impedance value of the order of 105-106 Ω/cm² was obtained at low and medium frequencies, suggesting good corrosion resistance for the thermal oxidation samples.

Figure 4 shows portions of resolved loops represent the Nyquist diagrams. This type of diagram is often interpreted as a charge transfer mechanism on an inhomogeneous surface [2]. It is observed for the three

thermally oxidized samples (TiOX). When thermal oxidation is applied, a tendency to increase the size of the capacitive loop (small picture) can be noticed, which can be attributed to the charge transfer process [12, 13].

Figure 4. Images shows (a) Nyquist and (b) Equivalent Circuit from EIS measurements.
 Figura 4. Las imágenes muestran en (a) Nyquist y en (b) Circuito equivalente de las mediciones del EIS.



Consequently, the naturally formed oxide film TiO_2 will have a higher resistance to corrosion but an easy transfer of the ions due to the thickness of this oxide film [14]. This phenomenon is well marked, and the impedance value obtained for the thermally oxidized samples (480°C, 560°C, and 640°C) tends to be higher than in the untreated sample (metallic base).

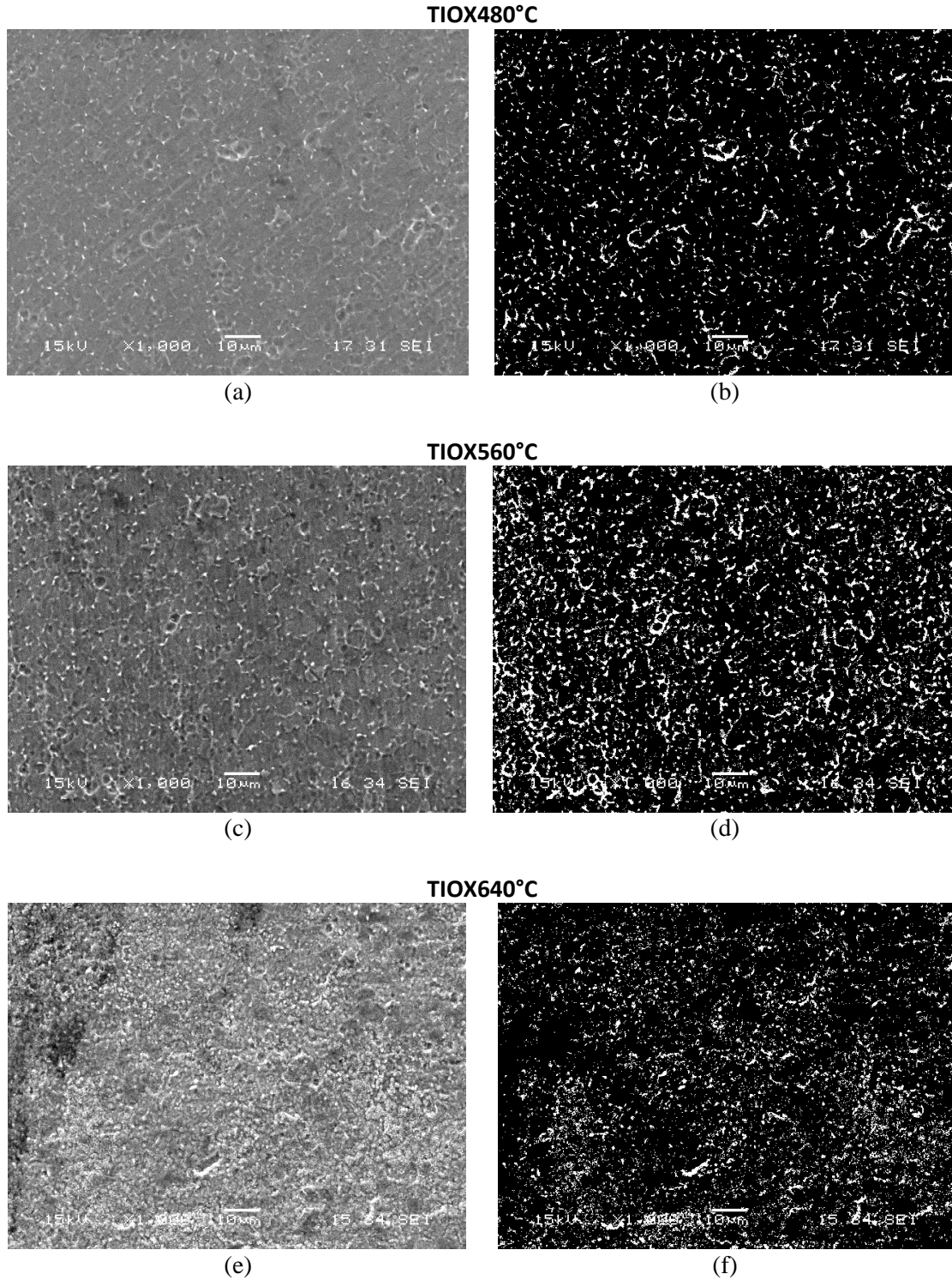
The above result reflects the influence of thermal oxidation in the Metal/ TiO_2 /Solution interface process and indicates a much higher corrosion resistance of the thermally oxidized samples.

3.3. SEM analysis and Image analysis

Figure 5 showed SEM and image analysis could characterize the surfaces of the samples evaluated after the corrosion process. From Figure 5, it is essential to highlight the white spots indicating the relationship between the first and second rows of Figure 5. For this purpose, thresholding is established to binarize the images based on their pixel contrasts and intensities. Otsu's thresholding allows obtaining a distribution of pixels correlated between contrast and intensities, for computing an automated threshold value for our experimentations in reference images $\text{TiOX}_{480^\circ\text{C}}$, $\text{TiOX}_{560^\circ\text{C}}$, and $\text{TiOX}_{640^\circ\text{C}}$ fixed thresholds in 0.5085. Finally, it is replaced by image pixels with white spots in those regions that exceed the defined threshold.

Figure 4. Surface morphologies – first row (a), (c), (e) after corrosion test and binarized images – second row (b), (d), (f).

Figura 4. Morfologías de la superficie - primera fila (a), (c), (e) después de la prueba de corrosión e imágenes binarizadas - segunda fila (b), (d), (f).



The surface of the sample, which exhibited maximum corrosion resistance, was still covered with TiO₂. The sample TiOX560°C had a higher TiO₂ porous layer (White Region). Corrosion results are associated with image analysis performed, indicating that a very stable oxide was formed on the surface and reflected in an increase in the thermally oxidized samples' corrosion resistance relative to the base metal. Registering that thermal oxidation processes accelerate the formation of TiO₂ porous layer.

5. CONCLUSIONS

Through thermal oxidation, it was evidenced that it accelerated the growth of the porous layer of TiO₂ in all the treated samples, thus increasing the corrosion resistance of all the samples.

The corrosion tests showed that the heat-treated samples presented corrosion potentials (E_{corr}) more remarkable than those of the base metal. The anodized sample of the alloy of Ti6Al4V at 560°C thermally oxidized presented better corrosion resistance than the other samples oxidized at different temperatures, which suggests that tests be carried out in a smaller range taking as a reference point the temperature of 560°C.

Digital image analysis using the OTSU method and its estimation of thresholds provided a novel way of estimating the percentages of the porous layers of TiO₂ and opens a possibility to estimate the formation of TiO₂ nanotubes in this type of procedure.

ACKNOWLEDGMENTS

The authors would like to acknowledge IMTEF- Research Group on Materials, Processes, and Manufacturing Technologies of the Universidad Autónoma del Caribe to support the development of this master's work. We are also grateful to Prof. Ph.D. Mercedes Cely for Anodizing Measurements.

REFERENCES

- [1] H. Guleryuz and H. Cimenoglu, "Effect of thermal oxidation on corrosion and corrosion–wear behaviour of a Ti–6Al–4V alloy," *Biomaterials*, vol. 25, pp. 3325-3333, 30 September 2004.
- [2] A. Farooq, A. Raza, A. Tayyeb, Q. Ahmad and R. Ahmad, "Electrochemical and Cell Response of Surface Modified Ti6Al4V for Biomedical Applications," *Journal of Bio- and Tribo-Corrosion*, pp. 1-8, 10 September 2019.
- [3] P. Roy, S. Berger and P. Schmuki, "TiO₂ Nanotubes: Synthesis and Applications," *A Journal of the German Chemical Society*, vol. 50, pp. 2904-2939, 21 March 2011.
- [4] N. Zakerin and K. Morshed-Behbahani, "Perspective on the passivity of Ti6Al4V alloy in H₂SO₄ and NaOH solutions," *Journal of Molecular Liquids*, vol. 333, no. 115947, pp. 1-12, 2021.
- [5] H. Juan, "Funcionalización superficial de aleaciones de titanio mediante anodizado para aplicaciones biomédicas," Universidad Autónoma de Madrid, Madrid, 2015.
- [6] B. Ribeiro, R. Offoiach, E. Rahimi, E. Saltin, M. Lekka and L. Fedrizzi, "On Growth and Morphology of TiO₂ Nanotubes on Ti6Al4V by Anodic Oxidation in Ethylene Glycol Electrolyte: Influence of Microstructure and Anodization Parameters," *Materials*, vol. 14, no. 10, pp. 1-15, 2021.
- [7] J. Yang, H. Yang, H. Yu, Z. Wang and X. Zeng, "Corrosion Behavior of Additive Manufactured Ti-6Al-4V Alloy in NaCl Solution," *Metallurgical and Materials Transactions A volume*, vol. 48, pp. 3583-3593, 6 April 2017.
- [8] S. Kumar, S. T. Narayanan, S.-G. Sundara and S. Seshadr, "Thermal oxidation of Ti6Al4V alloy: Microstructural and electrochemical characterization," *Materials Chemistry and Physics*, vol. 119, pp. 337-346, 5 September 2010.

- [9] S. Wang, Z. Liao, Y. Liu and W. Liu, "Influence of thermal oxidation temperature on the microstructural and tribological behavior of Ti6Al4V alloy," *Surface and Coatings Technology*, vol. 240, no. 2, pp. 470-477, 2014.
- [10] G. Longhitano, M. Arenas, A. Conde, M. Larosa, A. Jardini, C. Carvalho and J. Damborenea, "Heat treatments effects on functionalization and corrosion behavior of Ti-6Al-4V ELI alloy made by additive manufacturing," *Journal of Alloys and Compounds*, 25 June 2018.
- [11] S. Jelliti, C. Richard, D. Retraint, T. Roland, M. Chemkhi and C. Demangel, "Effect of surface nanocrystallization on the corrosion behavior of Ti-6Al-4V titanium alloy," *Surface & Coatings Technology*, pp. 82-87, 17 March 2013.
- [12] C. Ribeiro, A. Santos and A. de Sousa, "Cyclic Thermal Oxidation Evaluation to Improve Ti6Al4V Surface in Applications as Biomaterial," *Journal of Materials Engineering and Performance*, pp. 1-7, 24 July 2019.
- [13] C. M. Mercedes, G. Castellar, J. Pereira and R. Angel, "Efecto de la velocidad de calentamiento sobre las propiedades mecánicas y resistencia a la corrosión de aleaciones de titanio modificadas," *Ingeniare. Revista chilena de ingeniería*, vol. 26, no. 4, pp. 577-584, 2018.
- [14] C. Nava-Dino, C. López-Meléndez, R. Bautista-Margulis, M. Neri-Flores, J. Chacón-Nava, S. de la Torre, J. Gonzalez-Rodriguez and A. Martínez-Villafañe, "Corrosion Behavior of Ti-6Al-4V Alloys," *International Journal of Electrochemical Science*, pp. 2389-2402, 1 March 2012.
- [15] J. Fernandes, E. C. K.-K. Sherdil, R. Brito, G. Machado, S. Teixeira, J. Dupont and M. Leite, "Effect of anodisation time and thermal treatment temperature on the structural and photoelectrochemical properties of TiO₂ nanotubes," *Journal of Solid State Chemistry*, vol. 251, no. 1, pp. 217-223, 2017.
- [16] R. Romero and A. Rodríguez, "Evaluación de el efecto de la temperatura de anodizado sobre la respuesta tribológica de recubrimientos anódicos sobre la aleación Ti6Al4V," Universidad Industrial de Santander, Bucaramanga, 2012.